

# Optical cavity characterization in nanowires via self-generated broad-band emission

Adam M. Schwartzberg,<sup>1,2</sup> Shaul Aloni,<sup>1</sup> Tevye Kuykendall,<sup>1</sup> P. James Schuck,<sup>1</sup> Jeffrey J. Urban<sup>1,\*</sup>

<sup>1</sup>The Molecular Foundry, Lawrence Berkeley National Labs, Berkeley, CA 94720, USA

<sup>2</sup>Currently with Sandia National Labs, Livermore, CA 94551, USA

\*JJUrban@LBL.gov

**Abstract:** Broadband white light is of great spectroscopic value and would be a powerful tool for nanoscale spectroscopy, however, generation and direction of white light on this length scale remains challenging. Here, we demonstrate the generation of broadband white light in sub-wavelength diameter Gallium Nitride (GaN) wires by coincident one- and two-photon absorption mediated via defect states. This generation of broadband, “white” light enables single-nanowire interferometric measurements of the nanowires themselves via analysis of the Fabry-Pérot fringes that overlay the entirety of the emission spectrum. The quality factor and finesse of individual nanowire cavities were measured and calculated to be  $186 \pm 88$  and  $3.05 \pm 0.6$  respectively, averaged over 20 individual wires. This work presents a new, simple approach for the generation and direction of broad band white light at sub-diffraction limit length scales, ideal for translating classical white light spectroscopies to higher spatial resolutions than previously achieved.

© 2011 Optical Society of America

**OCIS codes:** (180.5810) Scanning microscopy; (190.3970) Microparticle nonlinear optics.

---

## References and Links

1. D. Psaltis, S. R. Quake, and C. Yang, “Developing optofluidic technology through the fusion of microfluidics and optics,” *Nature* **442**(7101), 381–386 (2006).
2. S. L. Chin, A. Brodeur, S. Petit, O. G. Kosareva, and V. P. Kandidov, “Filamentation and supercontinuum generation during the propagation of powerful ultrashort laser pulses in optical media,” *J. Nonlinear Opt. Phys. Mater.* **8**(1), 121–146 (1999).
3. M. A. Foster, A. C. Turner, M. Lipson, and A. L. Gaeta, “Nonlinear optics in photonic nanowires,” *Opt. Express* **16**(2), 1300–1320 (2008).
4. P. Schlotter, J. Baur, Ch. Hielscher, M. Kunzer, H. Obloh, R. Schmidt, and J. Schneider, “Fabrication and characterization of GaN/InGaN/AlGaIn double heterostructure LEDs and their application in luminescence conversion LEDs,” *Mater. Sci. Eng. B* **59**(1-3), 390–394 (1999).
5. S. Tanabe, S. Yoshii, K. Hirao, and N. Soga, “Upconversion properties, multiphonon relaxation, and local environment of rare-earth ions in fluorophosphate glasses,” *Phys. Rev. B Condens. Matter* **45**(9), 4620–4625 (1992).
6. P. J. Schuck, R. D. Grober, A. M. Roskowski, S. Einfeldt, and R. F. Davis, “Cross-sectional imaging of pendeo-epitaxial GaN using continuous-wave two-photon micro-photoluminescence,” *Appl. Phys. Lett.* **81**(11), 1984–1986 (2002).
7. J. F. Muth, J. H. Lee, I. K. Shmagin, R. M. Kolbas, H. C. Casey, B. P. Keller, U. K. Mishra, and S. P. DenBaars, “Absorption coefficient, energy gap, exciton binding energy, and recombination lifetime of GaN obtained from transmission measurements,” *Appl. Phys. Lett.* **71**(18), 2572–2574 (1997).
8. Y. Toda, T. Matsubara, R. Morita, M. Yamashita, K. Hoshino, T. Someya, and Y. Arakawa, “Two-photon absorption and multiphoton-induced photoluminescence of bulk GaN excited below the middle of the band gap,” *Appl. Phys. Lett.* **82**(26), 4714–4718 (2003).
9. Near band edge, Eg, of GaN ~3.1 eV (400 nm). This number is reduced from the strict band-edge value due to impurities and the exciton binding energy, ~20 meV,<sup>5</sup> in GaN.
10. Broad mid-gap state emission, centered at ~2.3 eV (540 nm), tapering off at ~1.2 eV (1  $\mu$ m).
11. T. Kuykendall, P. J. Pauzauskie, Y. Zhang, J. Goldberger, D. Sirbulu, J. Denlinger, and P. Yang, “Crystallographic alignment of high-density gallium nitride nanowire arrays,” *Nat. Mater.* **3**(8), 524–528 (2004).

12. Laser line throughput experiments are performed ratiometrically. First, transmission is measured from a top objective (100x, 0.95 NA air, Nikon), through a standard 150  $\mu\text{m}$  thick silica coverslip, and collected by a matching bottom objective and analyzed by spectrometer. Next, a GaN wire is aligned to the top objective via piezoelectric sample stage to maximize coupling and the bottom objective is aligned to the other end of the wire. The total counts collected through the GaN wire are corrected for differences in coupling between objective-objective and GaN-objective measurements.
13. S. Gradečak, F. Qian, H. G. Park, and C. M. Lieber, "GaN nanowire lasers with low lasing thresholds," *Appl. Phys. Lett.* **87**(17), 173111 (2005).
14. J. C. Johnson, H. Yan, P. Yang, and R. J. Saykally, "Optical Cavity Effects in ZnO Nanowire Lasers and Waveguides," *J. Phys. Chem. B* **107**(34), 8816–8828 (2003).
15. S. Ruhle, L. K. van Vugt, H. Y. Li, N. A. Keizer, L. Kuipers, and D. Vanmaekelbergh, "Nature of sub-band gap luminescent eigenmodes in a ZnO nanowire," *Nano Lett.* **8**(1), 119–123 (2008).
16. D. P. Lyvers, J. M. Moon, A. V. Kildishev, V. M. Shalae, and A. Wei, "Gold nanorod arrays as plasmonic cavity resonators," *ACS Nano* **2**(12), 2569–2576 (2008).
17. L. K. van Vugt, B. Zhang, B. Piccione, A. A. Spector, and R. Agarwal, "Size-dependent waveguide dispersion in nanowire optical cavities: slowed light and dispersionless guiding," *Nano Lett.* **9**(4), 1684–1688 (2009).
18. R. M. Ma, X. L. Wei, L. Dai, S. F. Liu, T. Chen, S. Yue, Z. Li, Q. Chen, and G. G. Qin, "Light coupling and modulation in coupled nanowire ring-Fabry-Pérot cavity," *Nano Lett.* **9**(7), 2697–2703 (2009).
19. A. E. Siegman, *Lasers* (University Science Books, 1986).
20. D. Kim, I. H. Libon, C. Voelkmann, Y. R. Shen, and V. Petrova-Koch, "Multiphoton photoluminescence from GaN with tunable picosecond pulses," *Phys. Rev. B* **55**(8), R4907–R4909 (1997).
21. J. W. P. Hsu, F. F. Schrey, and H. M. Ng, "Spatial distribution of yellow luminescence related deep levels in GaN," *Appl. Phys. Lett.* **83**(20), 4172–4174 (2003).
22. P. J. Pauzauskis, and P. Yang, "Nanowire photonics," *Mater. Today* **9**(10), 36–45 (2006).
23. S. Petit, D. Guennani, P. Gilliot, C. Hirlimann, B. Honerlage, O. Briot, and R. L. Aulombard, "Luminescence and absorption of GaN films under high excitation," *Mater. Sci. Eng. B* **43**(1-3), 196–200 (1997).
24. C. K. Sun, J. C. Liang, J. C. Wang, F. J. Kao, S. Keller, M. P. Mack, U. Mishra, and S. P. DenBaars, "Two-photon absorption study of GaN," *Appl. Phys. Lett.* **76**(4), 439–441 (2000).
25. The two photon absorption coefficient,  $\beta$ , was measured and approximated by first measuring an approximate two photon absorption. This is performed by measuring the total intensity of excitation light ( $I_0$ ), and the total integrated intensity of the band edge emission ( $I_{\text{PE}}$ ) assuming an approximate collection efficiency of 0.3%. Only the band edge emission is considered in this calculation as it is clearly due to a full two-photon absorption effect and can be assigned unambiguously. We assume a quantum yield of 100% and from this can obtain the post absorption intensity ( $I$ ). With this information we can obtain the two-photon absorption cross section ( $\sigma_2$ ) using the relation  $\sigma_2 = (I - I_0) / (I_0^2 \cdot \rho \cdot x)$  where  $\rho$  and  $x$  are density and path length respectively.  $\sigma_2$  is directly related to  $\beta$  by the relation  $\beta = (\rho \cdot \lambda \cdot \sigma_2) / (h \cdot c)$  where  $\lambda$  is the wavelength of light,  $h$  is Planck's constant, and  $c$  is the speed of light.
26. S. Gautier, G. Orsal, T. Moudakir, N. Maloufi, F. Jomard, M. Alnot, Z. Djebbour, A. A. Sirenko, M. Abid, K. Pantzas, I. T. Ferguson, P. L. Voss, and A. Ougazzaden, "Metal-organic vapour phase epitaxy of BInGaIn quaternary alloys and characterization of boron content," *J. Cryst. Growth* **312**(5), 641–644 (2010).
27. J. Wu, "When group-III nitrides go infrared: New properties and perspectives," *J. Appl. Phys.* **106**(1), 011101 (2009).

## 1. Introduction

Optical spectroscopy with nanoscale light sources is critical for realizing next-generation photonic devices such as in situ or "lab-on-a-chip" technologies [1]. Monochromatic light sources at this size regime ( $<1\mu\text{m}$ ) are straightforward to produce, however, many important spectroscopies, such as absorption, scattering, and white light interferometry require a broadband, directional, "white" light source. At present, no such directional nanoscale white light source exists. In principle, this is possible by directly translating the physics responsible for white light generation in micron-scale supercontinuum fibers (SCF) [2] to sub-wavelength structures. However, in practice, sub-micron SCF devices [3] are still critically limited by fabrication restrictions and the high power loads required which result in rapid deterioration and photodegradation. Here we report a novel approach to guided nanoscale white light generation based upon defect mediated efficient nonlinear upconversion and cascaded luminescence in gallium nitride (GaN) nanowires. This enables the use of low-power, sub-bandgap, continuous-wave (CW) illumination to produce the first directional, nanoscale white-light (WL) source pumped with sub-bandgap CW excitation.

One approach for the low-power generation of guided, nanoscale white-light (WL) requires simultaneously meeting two challenging criteria (shown schematically in Fig. 1): 1.)

broadband, multistate emission from one single structure and 2.) control over emission direction. The common solutions to WL generation, phosphorescent downconversion [4] and blackbody heating are not applicable at these length scales due to fabrication and material stability limitations, respectively. Here, upconversion of a wide band-gap, high index material with multi-state emission is utilized to produce a waveguided broadband nano-lightsource, as shown schematically in Fig. 1. First, by confining the structure responsible for broadband emission to a waveguide, we ensure that any light generation will result in directional emission, a requirement for spectroscopic applications. Ideally, such a waveguide should possess modest, but not exceptionally large, quality factor (Q) and finesse (F) values, as the goal is directed emission, not nanoscale lasing, where Q values are usually above 500 [3]. High light throughput and waveguiding are also desired, but power storage is not. Secondly, we will use mid-gap defect states as “bright” intermediate states to generate the upconverted light, similar to what is done in rare-earth doped oxides [5]. Moreover, as we are pumping nanoscale systems, avoidance of high photon flux and photodamage is crucial. Thus we limit ourselves to low power, continuous wave, visible excitation sources and, therefore, do not directly populate the band edge using UV excitation. We instead take advantage of the high two-photon absorption cross-section in GaN which will enable band-gap excitation of this wide-band gap ( $E_g \sim 3.1\text{ eV}$ , 400 nm) semiconductor using visible light, yielding broad emission ranging from the UV to the near-IR (NIR) [6,7].

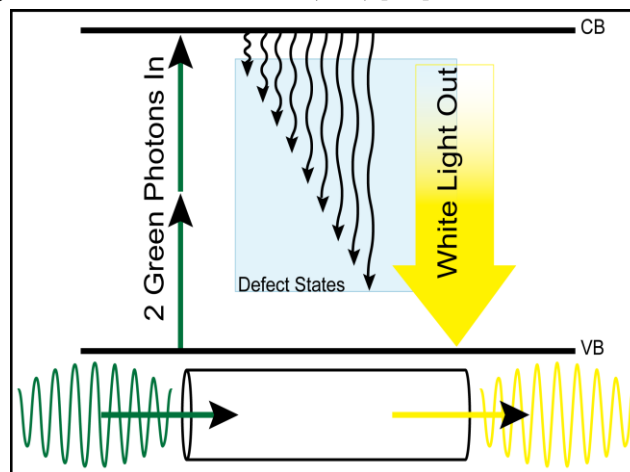


Fig. 1. Idealized schematic diagram of WL generation in a nanoscale waveguide (Bottom) via a two photon absorption followed by nonradiative decay to energetically broad mid-gap states and WL emission (Top).

WL photoluminescence (PL) observed in these GaN nanowires is attributed to a multi-step defect state mediated excitation process involving efficient coincident multiphoton upconversion, followed by near band-edge emission, as well as non-radiative decay into a wide energetic range of mid-gap luminescences, and direct emission from these states (i.e. the so-called blue-, green-, and yellow-band mid-gap states) [8]. These processes effectively produce contemporaneous and intense broadband emission spreading from the GaN band edge in the near UV [9] ( $\sim 2.95\text{ eV}$ , 420nm) into the visible ( $1.7\text{--}2.8\text{ eV}$ , 450-750nm) and near-IR [10] ( $\sim 1.4\text{ eV}$ , 900nm) regions of the spectrum, which, additively yield “white” light (with strong intensity and a symmetric emission profile from 1.4 to 3.0 eV, 400-900 nm). This result derives from the high density of mid-gap defect states in these GaN wires which efficiently mediate direct two-photon absorption to the band edge, creating an unusually high nonlinear absorption cross section, resulting in surprisingly facile upconversion and, ultimately, white light emission across the entire visible region of the spectrum.

## 2. Experimental

The GaN wires studied here are grown via MOCVD [11] and are crystalline with a faceted, triangular cross section, growing along the [120] direction. Samples were prepared by direct contact transfer onto  $\sim 150\text{ }\mu\text{m}$  glass coverslips from the as grown sapphire wafer containing large areas of vertically aligned wires. Photoluminescence (PL) and Raman measurements were performed on a WiTec alpha 300 S confocal microscope with both inverted and conventional objective orientations. All SEM comparison experiments were performed using a Nikon 100x 0.95 NA air objective. Other measurements were done with a Nikon 100x 1.4 NA oil immersion objective to maximize spatial resolution and minimize focal volume. Diode pumped solid-state lasers fiber coupled (Single mode, polarization maintaining (532 nm), and multi-mode (349 nm) fibers) into the microscope were used as excitation sources. The 532 nm laser (WiTec) was CW with a maximum power at the objective of 40 mW and the 349 nm laser (CrystaLaser) was Q-switched at 5 kHz with approximately 10 ns pulse width and a maximum power at the objective of  $\sim 5\text{ mW}$ . SEM was performed on a Zeiss Ultra 55 SEM in secondary electron collection mode at 1 kV acceleration.

## 3. Results and discussion

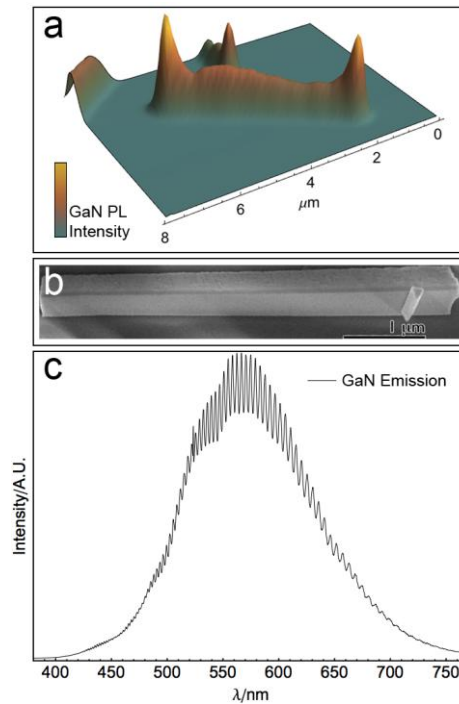


Fig. 2. Multi-photon confocal scanning emission image (a), SEM image of the corresponding wire (480 nm diameter) (b), and emission collected at the more intense end facets of the wire (c). Fringes overlaying the emission spectrum are Fabry-Pérot etalons of the GaN wire cavity.

In Fig. 2 we show a confocal PL image of a single GaN wire (Fig. 2a) and a scanning electron micrograph of the same wire (Fig. 2b). Distinct spikes in WL emission intensity, approximately three times greater than that of the wire body, are observed at the end facets of the wire indicating strong waveguiding of both the fundamental (pump frequency), as well as generated WL photons due to the significant index of refraction mismatch between GaN and air ( $n \sim 2.4$  and 1, respectively). The incident power of the focused pump laser (2.33 eV, 532 nm) is significant at the highest powers used (laser power: 38 mW, power density: 28

MW/cm<sup>2</sup>). The influence of this high photon flux is amplified by a high collection efficiency, whereby a large percentage (4-15% as shown by pump transmission experiments) of this light is transmitted through the wire at power densities of  $7.02 \pm 2.4$  MW/cm<sup>2</sup> through the entire wire [12]. Effectively, the laser focal volume is delocalized throughout the wire generating significantly greater WL emission. Wires of dimensions ranging from 50 – 600 nm in width were studied, however, below approximately 100 nm in width little waveguiding is observed.

Strikingly, photoluminescence studies reveal that this system produces broadband white light superimposed with Fabry-Pérot (FP) etalons over the entire recorded spectral range (Fig. 2c). This is notable because, while FP fringes have been observed in several other single nanoscale objects [13–18], in all instances those fringes have been observed only strongly at low-temperatures or under lasing conditions, and been of very narrow spectral range (~10-50 nm, ~80-400 meV)—these limitations in etalon behavior arise as they are constrained fundamentally by the bandwidth of the light used for analysis. Because this system uniquely generates broadband emission, we observe sharp and distinct FP etalons over an unprecedented spectral breadth (>250 nm, 1.8 eV) at room temperature; remarkable features which provide information regarding the optical properties of individual GaN nanowires and the quality of the GaN resonator cavity itself, free from ensemble averaging. The quality factor ( $Q$ ) and finesse ( $F$ ) of individual cavities, important parameters in understanding the waveguiding and light propagation properties of these nanoscale light sources, can be simply calculated by Eqs. (1) and (2).

$$Q = F * \frac{\lambda_r}{\Delta\lambda} \quad (1)$$

$$F = \frac{\Delta\lambda}{\delta\lambda} \quad (2)$$

Where  $\Delta\lambda$  is the spacing of the etalons,  $\delta\lambda$  is the full-width at half -maximum (FWHM) of the etalons, and  $\lambda_r$  is the wavelength of a particular etalon peak [19].

Measurements were made for over twenty wires, and average  $Q$  and  $F$  values were found to be  $186 \pm 88$  and  $3.05 \pm 0.6$  respectively, which are reasonable values for lossy resonators with unmirrored surfaces.  $Q$  values varied significantly from wire to wire with little correlation to wire width or PL intensity at end facets, but with a strong correlation to wire length. As  $Q$  is a measure of stored photon energy within the cavity, this is not an unexpected result, however, the degree of correlation is indicative of relatively poor reflectivity at the end facets. Cavities with highly reflective surfaces lose little light at each pass, and therefore the stored energy will remain relatively constant with length. This is immaterial to this particular system, however, as an intense, directional light source requires much of the light to escape the cavity, in contrast to an ideal CW laser cavity.  $F$  is directly dependent on resonator losses, and provides direct information about the properties of the end facets. As cavity end facet reflectivity is the dominant loss mechanism in such a system, we can determine an approximate geometric mean of the end facet reflectivity ( $R$ ) by Eq. (3).

$$R = 1 + 2 * \sin\left(\frac{\pi}{2F}\right)^2 - \frac{1}{2} \sqrt{-4 + \left(-2 - 4 * \sin\left(\frac{\pi}{2F}\right)^2\right)^2} \quad (3)$$

This yields an  $R$  of  $38 \pm 6\%$  (Derived from [19]). This is significantly higher than expected based on refractive index differences alone (~18%); yet, this corresponds to an 86.9% loss after a single round trip of photons within the cavity. While some portion of the light is resonating within the cavity, the majority of the emission observed at the end facets has only made a single trip within the waveguide.

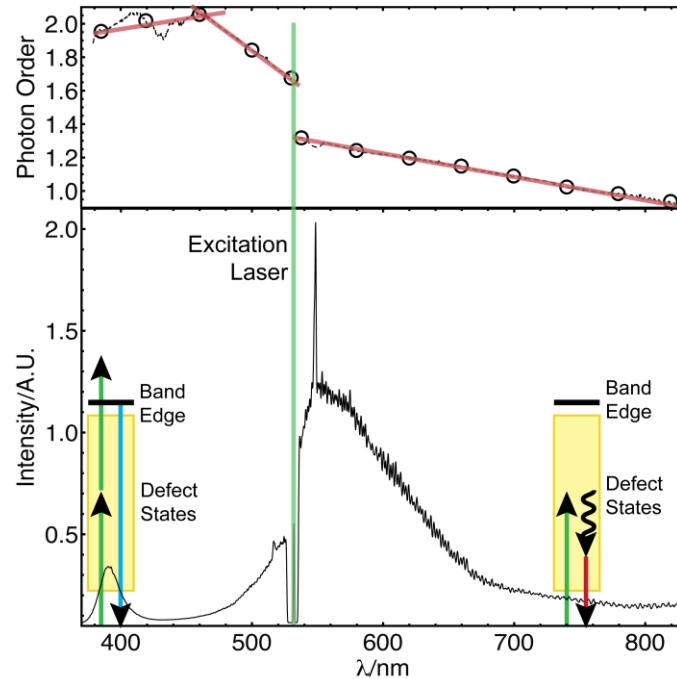


Fig. 3. Photon order spectrum over full emission window (top) and WL spectrum (bottom) of the same wire (380 nm diameter) at full power excitation (38 mW). At bottom left and right are schematic diagrams of two photon absorption and population of the band edge, and one photon absorption with population of mid-gap states, respectively.

Along with FP fringes, the emission spectral shape also provides insight into the nature of the WL generation. For example, the presence of similarly intense emission above and below the pump energy (2.33 eV, 532 nm) strongly indicates the participation of non-linear, multi-photon processes such as upconversion. Previous studies have indicated that two-photon absorption may result in emission blue-shifted from excitation [8,20,21], however, these studies are largely inconclusive and have all been conducted on bulk crystals or thin-film systems. While GaN nanowires in this size regime are not subject to quantum confinement, their nanoscale dimensions do give rise to distinct waveguiding properties and provide effective light-trapping [13,14,22].

Multi-photon absorption of emissive systems such as this is typically characterized by power-dependent emission intensity studies. By comparing the integrated emission intensity to the incident power density, a power law may be fit where the exponent reveals the photon order, or number of instantaneous photon absorption events responsible for the integrated emission. In Fig. 3 a photon order and emission spectrum of the same wire are shown (Note: close inspection of this spectrum clearly reveals FP fringes. However, due to the length of the wire, the spacing of the fringes is energetically very narrow ( $\sim 4$  meV at 500 nm), and at the presented energy range in Fig. 3 the individual oscillations are not clear). The photon order spectrum is obtained by determining the power dependence at each wavelength using only 2.33 eV (532 nm) excitation. The near band edge (2.95 – 3.26 eV, 380–420 nm) emission shows a two photon power dependence indicating the direct and simultaneous absorption of two green photons resulting in the population of band edge states and their resulting emission, as shown schematically at the bottom left of Fig. 3. There are likely direct contributions of mid-gap defect states in this two-photon absorption, as without this enhanced absorption, this process would likely be far too weak that the incident laser powers used at present. At the other end of the emission spectrum, near 1.55 eV (800 nm), the photon order decreases to one.



Previously, two-photon absorption coefficients ( $\beta$ ) for GaN have been shown to lie between 0.1 and 15 cm/GW [23,24]. By measuring total near band-edge emission intensity of  $\sim 500$  mW/cm<sup>2</sup> with 30 mW of pumping intensity we have measured an approximate  $\beta$  of 0.4 cm/GW for this portion of the spectrum [25]. This is a reasonable result, particularly considering the presence of two photon induced emission across much of the visible spectrum, not being taken into account in this measurement. To examine this further, visible (sub-band gap, 532 nm or 2.33 eV) and UV (supra-band gap, 349 nm or 3.55 eV) excitation of a single wire were compared, as shown in Fig. 4. As expected, near band edge PL is dominant with UV excitation, while WL mid-gap emission still dominates the spectrum with visible excitation. This result is even observed in wide field visible images taken of the wire under each illumination source. With UV illumination (Fig. 4, inset i), the emission appears purple as WL emission is de-enhanced, while visible illumination (Fig. 4, inset ii) produces an image of a completely different, white color. It should be noted that in addition to multi-photon arguments that may explain this data, saturation of defect states, which has been shown to enhance band-edge emission, is likely playing a large role. Moreover, this “enhanced” mid-gap emission with visible excitation, considered a detriment to many traditional GaN applications, is actually a productive advantage here, as the breadth, continuity, and intensity of our “white light” source derives from the highly-efficient illumination from these states. Figure 4b shows the color points of absolute white, and the GaN wires under UV and green illumination in the CIE 1931 color space. The blackbody emission color line is also shown. The color of the wire emission, while clearly not absolute white, is close to that of a 4000 K blackbody emitter, a neutral, full spectrum color. In comparison, UV pumped wires have a significantly bluer color point, significantly shifted from the blackbody emission line.

Emission from these nanowires is similar to UV-pumped phosphor based LEDs, however, with lower spectral intensity in the UV, producing a more “white” spectral response. This is a major advantage. There is some fluctuation in spectral features from wire to wire as seen by comparing spectra from Fig. 3 and Fig. 4, however, this will average out to a very broad spectrum when averaged over an ensemble of wires. The central advantage of using the nanowire upconversion to drive white light generation is precisely the lack of phosphors. This method eliminates all need for expensive phosphors and the attendant chemical processing needed to deposit them.

In general, multi-photon processes such as these typically require incredibly high peak-power light sources, such as femtosecond pulsed laser systems. Even in comparison to standard options for white light generation at the macroscale, this method of nanoscale white light generation is inexpensive, easy, highly reproducible, and insensitive to absolute wire dimensions. We use only a low power ( $\sim 40$  mW are used in attaining the above data, however, these effects can easily be observed well below 1 mW) CW laser source to pump the wires and obtain broadband white light without needing any expensive UV lasers or optics. The process is assisted by both the high two-photon absorption cross section in GaN [6] at our excitation wavelength, and also by the efficient waveguiding and light concentration intrinsic to this structure. The end facets of the wires are flat and parallel and act as effective broadband light resonators. We have estimated that, over a large portion of the observed spectrum, a single photon will make two to three round trip passes within the wire before exiting the cavity as emitted light. This light-trapping greatly increases the effective photon density in the wire, and the probability of two-photon interactions, as the upconversion seen here scale roughly with  $I^2$ , as anticipated. While the first reported generation of directed white light at this length scale, it has already been used to uncover new physical phenomena such as the emission power-dependence and the quality factor and finesse of individual wire cavities. This nanowire system offers a unique platform to truly translate the well-established fields of white-light spectroscopy and interferometry to the nanoscale, using simple, low-cost laser sources. In addition, it could be possible to utilize electroluminescence to drive nano-scale white-light emission in these wires, however, likely changes to the electrically driven



emission spectrum will require further characterization and development. Through further optimization of the optical properties of these wires, including doping with In-, P-, or B-, it may be possible to introduce some spectral tunability or enhanced emission intensity as well [26,27]. Such dopants act to shift the native bandgap to lower energies, allowing for lower energy two photon pumping ( $>700$  nm,  $<1.8$  eV) and lower energy defect states, shifting WL generation into the near-IR, further extending an already broad range of macro- and micro-scale spectroscopic techniques to the sub-wavelength spatial regime.

### **Acknowledgements**

Work at the Molecular Foundry was supported by the Office of Science, Office of Basic Energy Sciences, of the U.S. Department of Energy under Contract No. DE-AC02-05CH11231.